Multi-block and sequence-controlled polymerization of glycopolymers, and interaction with lectin

Kichize, Masaya
Department of Chemical Systems and Engineering, Kyushu University

Nagao, Masanori
Department of Chemical Systems and Engineering, Kyushu University

Hoshino, Yu
Department of Chemical Systems and Engineering, Kyushu University

Miura, Yoshiko
Department of Chemical Systems and Engineering, Kyushu University

出版情報：European Polymer Journal. 140 (110044), 2020-11-05. Elsevier
バージョン：
権利関係：

Multi-block and sequence-controlled polymerization of glycopolymers, and interaction with lectin

Masaya Kichize, Masanori Nagao, Yu Hoshino, and Yoshiko Miura

Department of Chemical Engineering, Kyushu University,
744 Motooka, Nishi-ku, Fukuoka, 819-0395, Japan

Corresponding author

Yoshiko Miura, miuray@chem-eng.kyushu-u.ac.jp

Abstract

Polymers with controlled molecular weights and sequences are expected to be functional polymers. Synthesis of multi-block glycopolymers were investigated to fabricate the functional biopolymers. The glycopolymers having mannose side chain with polyacrylamide backbone were polymerized with acrylamide derivatives. We synthesized of multi-block glycopolymers consisting of up to 9 blocks. The polymerization was conducted with rapid reaction in high yield. The multi-block glycopolymers with glycoblock at the both ends were prepared with narrow molecular weights dispersity. Molecular recognition of glycopolymers were analysed using mannose recognition protein of concanavalin A.

Keywords

Living radical polymerization, Reversible addition-fragmentation chain transfer polymerization (RAFT polymerization), Multi-block polymer, Polyacrylamide, Molecular recognition

Introduction

Biopolymers such as peptides and nucleic acids have precisely defined sequences, and exert their functions by adopting a three-dimensional structure derived from their primary sequence. Many research groups are currently focusing on mimicking biopolymers using synthetic polymers that can be easy to prepare, which has led to the development of a polymerization technique that can control both molecular weight and block sequence [1-4]. Living radical polymerization (LRP) has attracted significant attention owing to the versatile range of solvents and monomers that can be used [5-7]. By synthesizing the precise arrangements exhibited by biopolymers using radical polymerization, it is possible to prepare biomimetic material. LRP has made it possible to synthesize polymers with multi-block structures that can mimic the sequences of peptides and nucleic acids [1-2]. Perrier *et al.* successfully synthesized multi-block polymers using reversible addition fragmentation chain transfer (RAFT) polymerization an LRP technique [8-10]. Haddleton *et al.* used atom transfer radical polymerization (ATRP) to synthesize polymers in which two kinds of monomer are alternately arranged [11]. It is expected that the molecular weight and composition of synthetic polymers can be controlled by multi-block polymerization, and that biopolymers such as peptides and nucleic acids can be mimicked by functionalized multi-block synthetic polymers [12,13].

The arrangement of arbitrary functional groups based on the correct structures of biopolymers has been reported. Nanomaterials that introduce saccharides into peptides and nucleic acids and that utilize the molecular recognition properties of saccharides have been reported [14-16]. It is thought that in such studies the precisely defined sequence of the biopolymer is a platform, and the saccharide is a molecular recognition ligand. The function of the material can be controlled by tailoring the sequence of the ligands. The synthesis of precisely controlled synthetic polymers provides an inexpensive and stable alternative to biopolymers.

The Perrier group have reported multi-block copolymerization based on the fast kinetics of acrylamide [8] They showed sequence controlled polymerization of polyacrylamides by RAFT living based on the fast polymerization kinetics of acrylamide. Previously, we also reported the multi-block copolymerization of glycopolymer with a RAFT reagent based on the Perrier group's method [17]. The copolymerization of glucose-substituted acrylamide was studied, but the molecular recognition was not studied. In this study, the polymerization of glycopolymers with multi-block structures and mannose block at both ends were synthesized, and the molecular recognition with sugar recognition protein of

conncanavalin A (ConA) was studied, where the interaction between sugar and sugar recognition protein are genellay amplified by multivalent effect of glycopolymers.

2. *Experimental Section*

2.1 Materials.

2-Bromopropionic acid (98.0%), 3-(acetylthio)propionic acid (98.0%), 4-(4, 6-dimethoxy-1,3,5-triazin-2-yl)-4methylmorpholinium chloride (DMT-MM) (98.0%), sodium methoxide (96.0%), 4-acryloylmorpholine (98%), and *N,N*-dimethylacrylamide (99%) were purchased from Tokyo Chemical Industry (TCI) (Tokyo, Japan). 2,2'-Azobis[2-(2-imidazolin-2-yl)propane]dihydrochloride (VA-044) (98%), triethylamine (TEA) (99.0%), carbon disulfide (98.0%), and methanol dehydrate (dry MeOH) were purchased from Fujifilm Wako Pure Chemical Co. (Osaka, Japan). *D*(+)-Mannose, copper sulfate ($CuSO_4$) (97.5%), and sodium *L*-ascorbate (L-Asc Na) (98.0%) were purchased from Kanto Chemical (Tokyo, Japan). 2,2-Dimethyl-1,3-dioxolane-4-methanamine (97%) were purchased from Sigma-Aldrich (St. Louis, USA). The metal scavenger, SiliaMets Imidazole was purchased from SiliCycle Inc (Québec, Canada). Concanavalin A (ConA) was purchased from J-oilmils (Tokyo, Japan). Rabbit blood was purchased from Nippon Bio-test Laboratories Inc (Saitama, Japan). Mannose azide, *N*-(3-butynyl)acrylamide, and tris(benzyltriazolylmethyl) amine (TBTA) were prepared according to previous papers [17, 18]. Commercial including the radical inhibitor, 4-acryloylmorpholine and *N,N*-dimethylacrylamide were purified by passing through an alumina column before use.

2.2 Characterization.

Proton and carbon nuclear magnetic resonance (^{1}H NMR and ^{13}C NMR) spectra were recorded on a JEOLECP400 spectrometer (JEOL, Tokyo, Japan) using D_2O as a deuterated solvent. Size exclusion chromatography (SEC) with water as the solvent was performed on a JASCO DG-980-50 degasser equipped with a JASCO PU-980 pump (JASCO Co., Tokyo, Japan), a Shodex OHpak SB-G guard column, a Shodex OHpak SB-803 HQ column (Showa Denko, Tokyo, Japan) and a JASCO RI2031 Plus RI detector. SEC analyses were performed at a flow rate of 0.5 mL/min by injecting 20 µL of a polymer solution (1 g/L) in a 100 mM $NaNO_3$ aqueous solution. The SEC system was calibrated using a pullulan standard (Shodex). All the samples for SEC analysis were previously filtered through a 0.45 µm filter. Dynamic light scattering (DLS) was performed on a ZETASIZER NANO-ZS (Malvern, UK). The DLS analyses were

performed by using a 1 mL disposable cell of a polymer solution (1 mg/mL) in PBS buffer solution (pH 7.4). All the samples for DLS were previously filtered through a 0.45 µm filter. Mass spectroscopy of ESI-MS was measured with Waters ACQUITY system (Waters Co., USA).

*2.3 Preparation of mannose acrylamide derivative (MAm, **M**).*

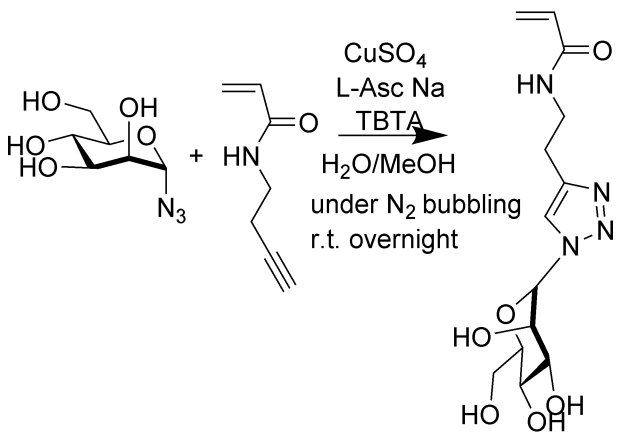

Scheme 1. Synthesis of an acrylamide derivative of *D*-mannose.

Acrylamide derivative of mannose (MAm, **M**) was synthesized with Huisgen cycloaddition (Scheme 1) [19, 20]. TBTA (0.461 g, 0.868 mmol) and $CuSO_4$ (0.139 g, 0.868 mmol) were dissolved in MeOH (44 mL)/H_2O (11 mL) mixture. A solution of mannose azide (1.78 g, 8.68 mmol) and 3-butynyl acrylamide (1.07 g, 8.68 mmol) in H_2O (11 mL) was added, and the oxygen was removed by bubbling nitrogen. *L*-Asc Na (0.344 g, 1.74 mmol) was added and stirred at room temperature overnight under nitrogen. The solution was concentrated under reduced pressure, and the precipitate was filtered. The crude product was purified by reverse-phase chromatography (Biotage SNAP ULTRA C18, gradient from water to methanol). The fraction containing the product was concentrated under reduced pressure and stirred with a metal scavenger 0.799 g) at room temperature overnight. After removal of metal scavenger of SiliaMets by filtration, the filtrate was concentrated under reduced pressure and the product was purified by reverse-phase chromatography again. The fraction was concentrated under reduced pressure and mannose acrylamide (MAm) product was obtained by freeze-drying (1.25 g, 44%).

^{1}H NMR (400 MHz, D_2O) δ in ppm: 2.87 (t, 2H, J=6.4 Hz, CO-NH_{amide}-CH_2-CH_2,), 3.09 (m, 1H, mannose H-5), 3.46 (t, 2H, J=6.4 Hz, CO-NH_{amide}-CH_2,), 3.64 (overlapped, 3H, mannose-H-6a,5,4), 3.95 (dd, 1H J=3.6 and 9.2 Hz, mannose H-3), 4.64 (overlapped, 2H, mannose H-6b,2,3), 5.57 (dd, 1H, J=2.0 and 7.6

Hz, vinyl(acrylamide)-*H*), 5.93 (d, 1H, J=1.8 Hz, mannose H-1), 5.98 (dd, 1 position 1H, J=2.0 and 15.2Hz, vinyl(acrylamide) -*H*), 6.05 (dd, 1H, J=15.2 and 15.2 Hz, vinyl(acrylamide) -*H*), 7.82 (s, 1H, C(triazole)-*H*).

^{13}C NMR(100 MHz, D_2O), δ in ppm: 24.5(*C*H_2-triazole), 38.7(*C*H_2-amide), 60.3, 66.5, 68.1,70.4, 75.9, 86.6(mannose), 123.3(triazole), 127.3(vinyl), 129.9(vinyl), 145.5(triazole), 168.5(carbonyl).

ESI-MS for C13H20N4O6 m/z: [M+Na]+ 351.14, found 351.28.

2.4 *General procedure of RAFT polymerization.*

Briefly, the monomer was dissolved in water with RAFT agent (DAOCTPA or the Macro-CTA) (Figure 1) and VA-044 [17]. The solution was degassed by freeze-thaw cycles (3 times) and placed in 70˚C water bath. The reaction was conducted with a sealed glass tube. The detail of reagents and solution volume were summarized in supporting information (Table S1). The reaction proceeded for 2 h at 70˚C. The reaction was stopped by exposing it to air. After polymerization, the solution was freeze-dried without purification, and the polymers were used for next polymerization step.

2.5 Hemagglutination inhibition assay (HI assay).

2.5.1 Blood preparation.

Rabbit blood was pelleted by centrifugation (2000 rcf × 5 min), and the layer of supernatant was removed by pipette. The blood was then diluted to 1 mL with PBS buffer (pH 7.4), the solution was centrifuged, and supernatant was removed by pipette. This process was repeated 3 times. The purified blood was diluted to 0.5 v/v% with PBS buffer.

2.5.2 ConA concentration titration of hemagglutination.

Polymers used were purified by dialysis (MWCO=3500). Rabbit blood solutions were incubated with the ConA solutions at each concentration to determine the ConA concentration required for hemagglutination. Serial two-fold dilutions were made in the wells of a 96 well V-bottomed plate. The two-fold dilutions were made by adding 100µL of ConA solution 1.0 mg/mL to the first well, then 50 µL of PBS buffer (pH 7.4) to the 2^{nd} – 12^{th} well (n=3). 50 µL was then transferred from the 1^{st} well to the 2^{nd} well. The 2^{nd} well was mixed and 50µL was transferred to the 3^{rd} well. This procedure was repeated until the 12^{th} well two-fold serial dilutions through all wells of interest. To each well 50µL of the blood

solution was added and incubated for 1 h at room temperature. Precipitation of blood cells was confirmed at the bottom of the well, and the amount of ConA required for hemagglutination was determined as hemagglutin units. Hemagglutinin unit was used for measuring the minimum inhibition concentration of hemagglutination.

2.5.3 Measurement of minimum inhibition concentration of the hemagglutination by glycopolymers.

Starting with a concentration of 2 mg/mL, serial two-fold dilutions of each glycopolymer (**$M_{20}D_{20}A_{20}D_{20}M_{20}$**, **$M_{20}(D_{20}A_{20})_2D_{20}M_{20}$**, **$M_{20}(D_{20}A_{20})_3D_{20}M_{20}$**, **$M_{20}$**, **$M_{120}$**, **MAm**, and **Mannose**) were made as described above (25 μL solution in 1^{st} ~ 12^{th} well). The glycopolymer solutions were incubated with 25 μL of the ConA solution for 1 h at room temperature. Then, 50 μL of the blood solutions was added and incubated for 2 h at room temperature. Precipitation of red blood cells was confirmed at the bottom of the well, and minimum concentration causing inhibition was determined by naked eyes.

3. Result and Discussion

3.1 Preparation of multi-block glycopolymer

Acrylamide type of monomers were used in this study. Accrylamide carrying mannose (MAm, **M**); *N,N*-dimethylacrylamide (DMA, **D**); and 4-acryloylmorpholine (AMP, **A**) were used as monomers. MAm was used as sugar monomer, which specifically bind to the mannose recognition protein of ConA. DMA and AMP were used as monomers for spacer segment to arrange sugars. Aqueous RAFT agent 2-(((((3-(2,3-dihydroxypropyl)-amino)-3-oxopropyl)thio)carbonothioyl)thio)-propanoic acid (DAOCTPA) was used as a chain transfer agent in water [17], and the initiator was VA-044. 10-hour half-life temperature of VA-044 is 44 ° C, and VA-044 is used for the quick initiation within 2h polymerization [8]. The target degree of polymerization (D.P.) of each block was 20, and MAm was polymerized in the first and last blocks to position saccharides at both ends (Figure 1)

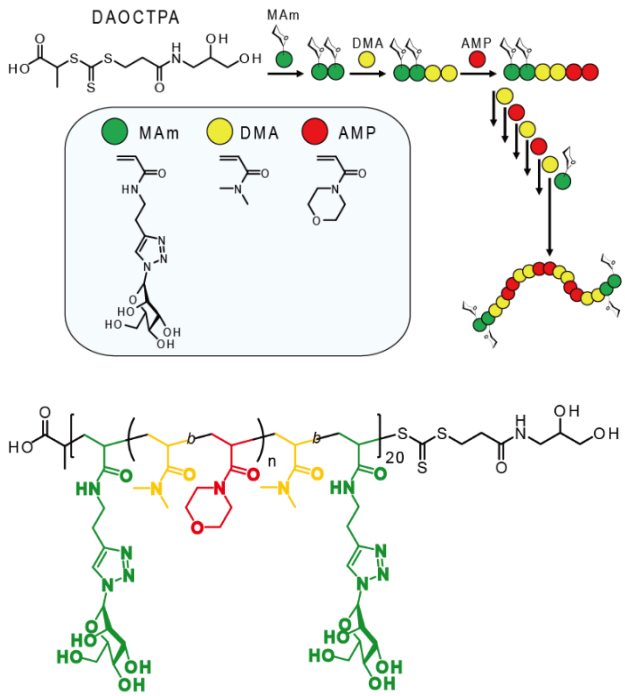

Figure 1 Schematic illustration of synthesis of multi-block glycopolymer.

The polymerization was allowed to proceed in water at 70 °C for 2 h. A block polymer with five blocks in which AMP and DMA were arranged between saccharide blocks was synthesized (**$M_{20}D_{20}A_{20}D_{20}M_{20}$**). The monomer concentration ([M]) and the feed ratio of the monomer to chain transfer agent and initiator ([M]: [CTA]: [I]) in each polymerization step are shown in Table 1. The equivalent amount of initiator to CTA was 0.01 eq for DMA and AMP, and 0.02 eq for MAm. ^{1}H NMR measurement following each polymerization step showed no peak derived from the vinyl group of the monomer (6.0 ~ 6.5 ppm), and the conversion of the monomer was >99%, which was determined by the disappearance of vinyl group (Figure 2(a)). The number average molecular weight (M_n) and molecular weight dispersity index (M_w/M_n) of the polymers after each polymerization step were determined by size exclusion chromatography (SEC) analysis. The values of M_n and molecular weight dispersity increased gradually with the elongation of the blocks. The value of dispersity was below 1.4 after the 5th polymerization step. In addition, the SEC trace showed unimodal peaks (Figure 2(b) and (c)). The hydrodynamic diameter D_h of the synthesized polymer was measured using dynamic light scattering (DLS), and the D_h was found to increase with the extension of the block structure (Table 1). Complete consumption of the

monomer was confirmed by ^{1}H NMR measurement, and the monomers were quantitatively introduced into the polymer structure. The unimodal SEC analysis peaks and the increase of the D_h determined by DLS indicated that the polymerization proceeded as a block polymerization. The relatively low dispersity demonstrated that the polymer structure was well-controlled.

Glycopolymers having mannose group at each end [$\mathbf{M_{20}(D_{20}A_{20})_2D_{20}M_{20}}$ and $\mathbf{M_{20}(D_{20}A_{20})_3D_{20}M_{20}}$] were also synthesized and were characterized by SEC and DLS (Figure 2(d)). The SEC analysis showed that each peak was unimodal and that the trace was clearly divided as a result of the difference in the number of blocks present in each polymer. The D_h values for $\mathbf{M_{20}D_{20}A_{20}D_{20}M_{20}}$, $\mathbf{M_{20}(D_{20}A_{20})_2D_{20}M_{20}}$, and $\mathbf{M_{20}(D_{20}A_{20})_3D_{20}M_{20}}$ were 5.50, 6.37, and 7.37 nm, respectively. The difference in the number of internal blocks controlled the arrangement of the saccharide blocks at both ends of the polymers [21]. Homo-glycopolymers ($\mathbf{M_{20}}$ and $\mathbf{M_{120}}$) consisting only of MAm were synthesized for comparison with the multi-block glycopolymers in the interaction evaluation. The polymerization was performed under the same conditions as for the synthesis of the multi-block glycopolymers.

Polymers were obtained with narrow dispersity, suggesting the success living radical polymerization. The polymerization kept narrow dispersity even after 9th polymerization. Though the dispersity became a little larger with each polymerization step, the dispersity was below 1.50, showing the controlled polymerization with a bulky sugar monomer. The hydrodynamic diameters of the polymers showed the polymer size was increased by the polymer elongation. The polymer size was monotonously increased with polymerization with DP less than 100 mer, suggesting the possibility of control the molecular structure [22]. In each step, the monomer conversion was high, and the total yield of 9 step polymerization was 81 %

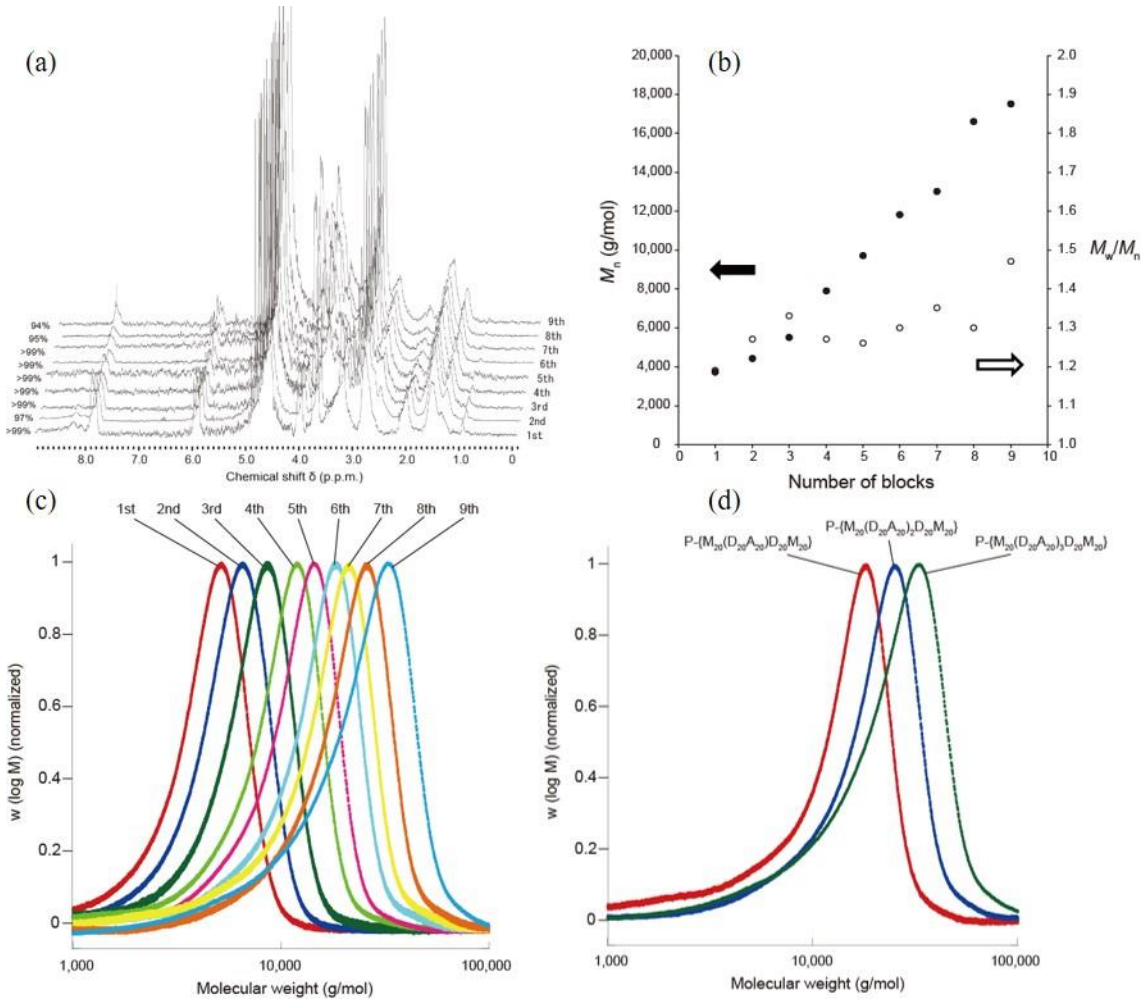

Figure 2 (a) ^{1}H NMR spectra (400 MHz, D_2O) showing the monomer conversion for each block after 2 h of RAFT polymerization. (b) Evolution of the relative molecular weights and molecular weight dispersity with number of blocks for the preparation of multi-block glycopolymer. Full circles represent the molecular weight from SEC analysis, and empty circles represent the molecular weight dispersity. (c) SEC chromatograph of the bock glycopolymers after each polymerization step (solvent: 100 mM $NaNO_3$ aq). (d) SEC chromatograph of the multi-block glycopolymers (solvent: 100 mM $NaNO_3$ aq).

Table 1. Properties of RAFT polymerization for preparation of multi-block glycopolymer.

	Target Polymer structure[a]	[M]: [CTA]: [I]	Conv (%)[b]	D.P. (mer)[c]	$M_{n,the}$ (g/mol)[d]	$M_{n,SEC}$ (g/mol)[e]	M_w/M_n [e]	D_h (nm)[f]
1	M_{20}	20:1:0.02	>99	20	6,900	3,700	1.19	2.83
2	$M_{20}D_{20}$	20:1:0.01	97	40	8,900	4,400	1.27	3.80
3	$M_{20}(D_{20}A_{20})$	20:1:0.01	>99	60	11,700	5,500	1.33	4.40
4	$M_{20}(D_{20}A_{20})D_{20}$	20:1:0.01	>99	81	13,800	7,900	1.27	4.67
4-2[g]	$M_{20}(D_{20}A_{20})D_{20}$ M_{20}	20:1:0.02	>99	100	20,000	10,800	1.35	5.50
5	$M_{20}(D_{20}A_{20})_2$	20:1:0.01	>99	100	16,500	9,700	1.26	5.31
6	$M_{20}(D_{20}A_{20})_2D_{20}$	20:1:0.01	>99	120	18,400	11,800	1.30	5.76
6-2[g]	$M_{20}(D_{20}A_{20})_2D_{20}$ M_{20}	20:1:0.02	>99	139	24,600	15,700	1.32	6.37
7	$M_{20}(D_{20}A_{20})_3$	20:1:0.01	>99	139	21,100	13,000	1.35	5.88
8	$M_{20}(D_{20}A_{20})_3D_{20}$	20:1:0.01	95	160	23,200	16,600	1.30	6.52
9[g]	$M_{20}(D_{20}A_{20})_3D_{20}M_{20}$	20:1:0.02	94	179	29,400	17,500	1.47	7.37
10	M_{120}	120:1:0.04	>99	119	39,300	18,200	1.20	7.07

a) The monomer, MAm, DMA, and AMP were abbreviated to M, D, and A in the polymer structure, respectively. b) Monomer conversion (Conv.) was determined by ^{1}H NMR measurement. c)Degree of polymerization (D.P.) was determined from ^{1}H NMR measurement. d) $M_{n,\,the}$ = $MW_{monomer}$ × D.P. + MW_{CTA}. e) Molecular weight and molecular weight dispersity index were determined by SEC analysis. The eluent was 100 mM $NaNO_3$ (aq), and the sample calibrated with pullulan standard. f) The hydrodynamic diameter (D_h) was determined by DLS measurement (1 mg/mL in HEPES buffer).g)Glycopolymers having mannose at both ends.

3.2 Interaction of glycopolymers with sugar recognition protein

The interaction of the three multi-block glycopolymers - **$M_{20}D_{20}A_{20}D_{20}M_{20}$**, **$M_{20}(D_{20}A_{20})_2D_{20}M_{20}$**, and **$M_{20}(D_{20}A_{20})_3D_{20}M_{20}$** - with the target protein (ConA) was evaluated. The evaluation was carried out using a hemagglutination inhibition assay (HI assay) (Figure 3) [23]. ConA is a protein that recognizes mannose, and was selected as a target protein because of the well-defined tetrameric structure [24-26]. ConA has four sugar recognition sites at each vertex. The sugar concentration for erythrocyte inhibition was measured. The inhibition constant (K_i) of the sample was determined by the lowest inhibition concentration. A smaller K_i value represents a stronger interaction. The K_i of **$M_{20}D_{20}A_{20}D_{20}M_{20}$**, **$M_{20}(D_{20}A_{20})_2D_{20}M_{20}$**, **$M_{20}(D_{20}A_{20})_3D_{20}M_{20}$**, **$M_{20}$**, and **$M_{120}$** were 9.88, 10.6, 13.4, 12.7, and 6.34 ($\times 10^{-4}$ M), respectively. MAm, mannose and polymers without mannose did not inhibit the hemagglutination.

The interaction of the glycopolymers with ConA was amplified by multivalent effect in all polymers. Among them **M_{120}** showed the strongest interaction, and the K_i of **M_{120}** was 2 times smaller than that of **M_{20}**. **M_{120}** has ability to bind to two binding sites of ConA because the D_h of **M_{120}** (6.90 nm) was larger than 6.50 nm – the distance between the sugar binding sites of ConA [25]. In constant, since the D_h of **M_{20}** was 2.83 nm, which is smaller than 6.5 nm, **M_{20}** was thought to bind to one ConA binding site. The difference in the number of binding sites influenced the interactions of **M_{20}** and **M_{120}** with ConA [21, 26, 27]. The detailed molecular recognition of these polymers is currently in under investigation.

The interactions of the multi-block glycopolymers with saccharides at both ends with ConA were almost the same as that of **M_{20}**. Since the D_h values of **$M_{20}(D_{20}A_{20})_2D_{20}M_{20}$** and **$M_{20}(D_{20}A_{20})_3D_{20}M_{20}$** were larger than 6.5 nm, these glycopolymers were expected to exhibit the same degree of interaction as **M_{120}**. However, the K_i values of the three polymers - **$M_{20}D_{20}A_{20}D_{20}M_{20}$**, **$M_{20}(D_{20}A_{20})_2D_{20}M_{20}$**, and **$M_{20}(D_{20}A_{20})_3D_{20}M_{20}$** - were relatively consistent. Our group has previously reported that the interaction of methacrylate type triblock glycopolymers with ConA could be controlled by tailoring the distance between the saccharide blocks [21] . The binding affinity of glycopolymers were also conducted by florescence quenching experiment with FITC-ConA (supporting information Figure S8). The weak binding affinity of multi-block glycopolymers, comparing **M_{120}**, were also confirmed by fluorescence quenching method.

The previous results of our glycopolymer and the currents results of multi-block glycopolymers were not consistent [21]. In the previous report, a glycopolymer having mannose segments at both ends showed the strong interaction to ConA based on the bivalent interaction. However, the similar glycopolymer in the current research did not show the strong interaction. If the binding of glycopolymers are determined only by the sugar display, the ConA binding ability of $\mathbf{M_{20}(D_{20}A_{20})_3D_{20}M_{20}}$ would be much stronger than $\mathbf{M_{20}D_{20}A_{20}D_{20}M_{20}}$ and similar to $\mathbf{M_{120}}$ because sugar can reach two mannose binding site**,** but vice versa. These results suggested that the sugar-protein interaction was determined not only by sugar spatial display, but also by other factors like physical properties of polymers and hydrophobicities [27, 28]. The previous glycopolymers had polymethacrylate backbone, and the current glycopolymers have polyacrylamide backbone, where the difference in polymer backbone result in the different properties.

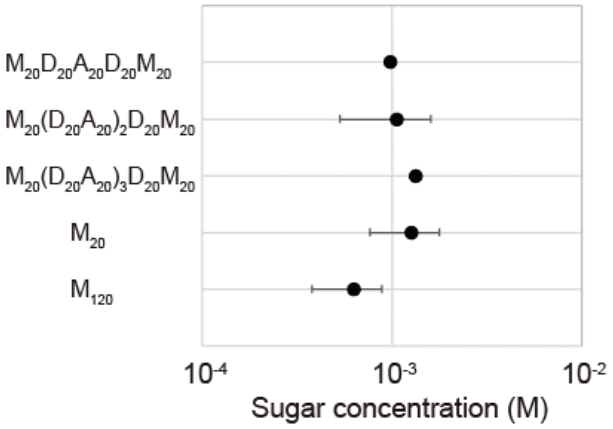

Figure 3. K_i plots from HI assay of the multi-block glycopolymers (n = 3).

4. Conclusion

We synthesized multi-block glycopolymers with well-defined sequence and narrow molecular weight dispersity with fast reaction and high yield, by optimized RAFT living radical polymerization. Although a glycomonomer having mannose side chain are bulky and multiblockpolymers have complex molecular structures, all polymers were obtained in high yield in this study. The analysis of polymers by SEC and DLS revealed that the polymers are prepared based on the molecular design. Molecular recognition ability of glycopolymers was maintained

even in multi-block polymers with complex structures. The synthesis technology of these polymers will be useful for the progress of biomaterials and biotechnology.

Acknowledgement

This study was supported by the Grant-in-Aid for Scientific Research B (JP19H02766), Grant-in-Aid for Challenging Research (Pioneering) (JP19K22971), Grant-in-Aid for Scientific Research on Innovative Areas (JP20H05230 and JP20H04825), and Eno scientific foundation.

References

[1] Hoshino Y, Koide H, Furuya K, Haberaecker WW, Lee SH, Kodama T, Kanazawa H, Oku N, Shea KJ, Proc. Natl. Acad Sci USA 2012;109:33-38.

[2] Wada Y, Lee H, Hoshino Y, Kotani S, Shea KJ, Miura Y, J. Mater. Chem. B 2015;3: 1706-1711.

[3] Gutekunst WR, Hawker CJ, J. Am. Chem. Soc. 2015; 137: 8038-8041.

[4] Lavilla C, Byrne M, Heise A, *Macromolecules* 2016; 49: 2942-2947.

[5] Lutz JF, Lehn J, Meijer EW, Matyjaszewski K, *Nat. Rev. Mater.*2016; 1: 16024.

[6] Lutz JF, Ouchi M, Liu DR, Sawamoto M, *Science.* 2013; 341: 1238149.

[7] Perrier S, *Macromolecules* 2017; 50: 7433-7447.

[8] Gody G, Maschmeyer T, Zetterlund PB, Perrier S, *Nature. Communication.*, 2013; 4: 2505.

[9] Martin L, G. Gody G, Perrier S, *Polym. Chem.*, 2015; 6: 4875-4886.

[10] Gody G, Barbey R, Daniel M, Perrier S, *Polym. Chem.*, 2015; 6: 1502-1511.

[11] Zhang Q, Collins J, Anastasaki A, Wallis R, Mitchell DA, Becer CR, Haddleton DM, *Angew. Chem.*2013; 125: 4531-4535.

[12] Engelis NG, Anastasaki A, Nurumbetov G, Truong NP, Nikolaou V, Shegiwal A, Whittaker MR, Davis TP, Haddleton DM., *Nature. Chemistry.* 2017; 9: 171-178.

[13] Nurumbetov G, Engelis N, Godfrey J, Hand R, Anastasaki A, Simura A, Nikolaou V, Haddleton DM, *Polym. Chem.* 2017; 8: 1084-1094.

[14] Hasegawa T, Sasaki T, *Chem. Commun.* 2003; 978-979.

[15] Matsuura K, Hibino M, Yamada Y, Kobayashi K., *J. Am. Chem. Soc.* 2001; 123: 357-358.

[16] Waldmann M, Jirmann R., Hoelscher K., Wienke M., Niemeyer FC, Rehders D, B. Meyer B, *J. Am. Chem. Soc.* 2014; 136: 783-788.

[17] M. Nagao M, Hoshino Y, Y. Miura. Y, *J. Polym. Sci. Part A: Polym. Chem*, 2019, 57, 857-861.

[18] Tanaka T, Nagai H, Noguchi M, Kobayashi A, Shoda S, *Chem. Commun.* 2009; 3378-3379.

[19] Rostovtsev VV, Green LG, Fokin VV, Sharpless KB, *Angew. Chem. Int. Ed. Engl.*, 2002; 41: 2596.

[20] Tornoe CW, Christensen C, Meldal M, *J. Org. Chem.*, 2002; 67: 3057-3064.

[21] Jono K, Nagao M, Oh T, Sonoda S, Hoshino Y, Miura Y., *Chem. Commun.* 2018; 54: 82-85.

[22] Yoshida N, Yoshizaki T, Yamakawa H, *Macromolecules*, 2000; 33: 3252-3258.

[23] Nagao M, Fujiwara Y, Matsubara T, Hoshino Y, Miura Y, *Biomacromolecules*, 2017; 18: 4385-4392.

[24] Lundquist JJ, Toone EJ, *Chem. Rev.* 2002; 102: 555-578.

[25] Hardman KD, Ainsworth CF, *Biochemistry* 1972;11: 26, 4910-4919.

[26] Gestwicki JE, Cairo CW, Strong LE, Oetjen KA, Kiessling LL, *J. Am. Chem. Soc.* 2002; 124: 14922-14933.

[27] Gerke C, Ebbesen MF, Jansen D, Boden S, Freichel T, Hartmann L, *Biomacromolecules* 2017; 18: 787-796.

[28] Dimick SM, S. C. Powell SC, S. A. McMahon SA, D. M. Moothoo DM, J. H. Naismith JH, E. J. Toone Ej, *J. Am. Chem. Soc.* 1999; 121: 44: 10286-10296.

[29] Hoshino Y, Nakamoto M, Miura Y. *J. Am. Chem. Soc.* 2012; 134: 15209-15212.

[30] Nagao M., Matubara T, Hoshino Y, Sato T, Miura Y, *Biomacromolecules*, 2019; 20: 2763-2769.